Flow Over a Thin Needle Moving in a Casson Fluid

D. SRINIVASACHARYA*, G. SARITHA
Department of Mathematics, National Institute of Technology Warangal,
Hanumakonda 506 004, Telangana,
INDIA

**Corresponding Author*

Abstract: - This study examines the boundary layer flow across a thin, horizontal needle moving in a Casson fluid. The underlying equations are initially converted into a set of ordinary differential equations using similarity transformations, and thereafter successive linearization is applied. The Chebyshev collocation technique is applied to find the solution of the linearized equations. The temperature and velocity profiles, together with the skin friction coefficient and the Nusselt number, are illustrated graphically for different values of the needle size and Casson fluid parameter.

Key-Words: - Boundary Layer flow, Casson fluid, Thin needle, Similarity transformations, Heat transfer rate, Skin friction coefficient, Successive linearization, Chebyshev collocation method.

Received: April 25, 2023. Revised: November 15, 2023. Accepted: January 14, 2024. Published: April 1, 2024.

1 Introduction

Several investigators have been examining the flow and heat transfer in different geometries, such as a flat plate, stretching sheet, horizontal cylinder, stretching cylinder, disc, stretching disc, sphere, elastic sheet, etc. Applications for the flow and heat transmission corresponding to a thin needle can be found in a wide range of fields, including biomedicine, microstructure electronic tools, hot wire anemometers, lubrication and power generation, aerodynamics, blood flow, microscale cooling devices, cancer therapy, wire coating, and many more. Thin needle geometry refers to the smearing surface produced by rotating a parabola around its axis. [1], was the first to introduce a boundary layer flow across a tiny moving needle in a parallel free stream. Thereafter, the similarity solutions for convective flow over a needle were presented in [2], [3], [4]. The forced laminar convective nanofluid stream past a horizontal needle was analysed in [5]. The flow around a small needle with changeable viscosity and thermal conductivity was examined in [6]. The consequences of hybrid nanoparticles on the flow across a hot needle has been reported in [7]. In a fluid containing hybrid nanoparticles, [8] studied the influence of viscous dissipation, magnetic fields, and radiation on fluid flow across a moving needle.

The study of non-Newtonian fluid flow attracted the interest of several researchers due to its relevance to a wide range of engineering problems. These include tarry fuel abstraction from petroleum-based goods, the manufacture of plastic materials, crystal growth, the freezing of nuclear reactors, etc. Further, the boundary layer flow of non-Newtonian fluid around the thin needle has important physical practical applications such as in marine structures and marine vehicles, torpedoes, water towers, bridges, and many more. There is no single fluid model that can accurately describe the properties of non-Newtonian fluids. As a result, various fluid models were described in the literature over the previous century to explain real fluid dynamics. [9], presented the Casson fluid model, which is a shear-thinning fluid. The viscosity of these fluids is infinite at no shear rate and non-existent at infinite shear rates. It is worth noting that if the yield stress is less than the shear stress, this model reduces to a Newtonian liquid. It offers an easy way to calculate the two parameters, Casson viscosity, and apparent yield stress, for use in real-world applications. In recent years, the Casson fluid model has been employed in a variety of theoretical and computational studies due to its extensive applicability in drilling operations, metallurgy, food processing, polymer processing industries, synthetic lubricants, biomedical fields, the preparation of printing ink, etc. Although Casson fluid flow across a thin needle is significant, very little research has been published. The influences of radiation and cross diffusion on the magnetic Casson nanofluid along a needle were scrutinized by [10]. [11], analyzed the MHD effects on the Casson fluid with nanoparticles over a thin needle. The thermally radiative magnetic Casson fluid with nanoparticles on the needle under the Navier-Slip

effect has been explored in [12]. In the presence of internal heat and nonlinear thermal radiation, [13], examined the Casson fluid flow with nanoparticles around a thin needle. The influence of injection, temperature-dependent viscosity, and thermal conductivity on the natural convection Casson fluid flow from a spinning cone in a porous medium were considered in [14]. The consequence of Soret effect and viscous heating with thermal and solutal dispersion on the double diffusion convection Casson fluid flow along a vertical plate was analysed by [15]. The hydromagnetic flow of Casson nanofluid in Armory production was considered by [16].

This work considers the steady flow of a Casson fluid along a horizontal, thin needle. The flow equations are initially converted into a set of ordinary differential equations, then linearized by applying successive linearization and solved via the Chebyshev collocation technique.

2 Problem Formulation

Consider the flow of Casson fluid with uniform velocity U_∞ over a thin needle moving horizontally with a velocity U_w. Assume that flow is steady, laminar, and incompressible. The coordinate system and schematic of the problem is shown in Figure 1. The equation for the radius of the needle is r = R(x). It is supposed that the needle is thin while the needle's thickness is less than that of the boundary layer surrounding it. The temperature of the needle is T_w, whereas the temperature of the surrounding fluid is T_∞, where $T_w > T_\infty$ and $C_w > C_\infty$.

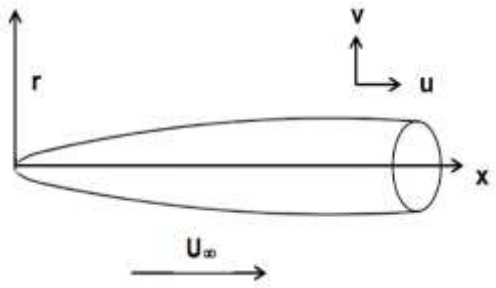

Fig. 1: "Coordinate system and physical flow model"

With the above assumptions and invoking boundary layer postulations, the flow equations are:

$$\frac{\partial}{\partial x}(ur) + \frac{\partial}{\partial r}(vr) = 0 \quad (1)$$

$$\left(\rho u \frac{\partial u}{\partial x} + \rho v \frac{\partial u}{\partial r}\right) = \frac{\mu}{r}\left(1 + \frac{1}{\beta}\right)\frac{\partial}{\partial r}\left(r \frac{\partial u}{\partial r}\right) \quad (2)$$

$$u \frac{\partial T}{\partial x} + v \frac{\partial T}{\partial y} = \frac{\alpha}{r}\frac{\partial}{\partial r}\left(r \frac{\partial T}{\partial r}\right) \quad (3)$$

where u and v denote the axial and redial velocity components, T represents the fluid temperature, μ represents the viscosity, β represents the Casson fluid parameter, ρ represents the fluid density and α represents the thermal conductivity.

The conditions on the surface of the needle are:

$v = 0$, $T = T_w$, $u = U_w$ $C = C_w$ at r=R(x)

$T \to T_\infty$, $u \to u_\infty$, $C \to C_\infty$ at $r \to \infty$ (4)

The similarity transforms are defined as:

$$\Psi = vx\lambda f(\eta),\ \theta(\eta) = \frac{T - T_\infty}{T_w - T_\infty},\ \ \eta = \frac{Ur^2}{vx} \quad (5)$$

where $U = U_w + U_\infty$ is the composite velocity and Ψ is stream function.

If the equation $\eta = a$, where 'a' is dimensionless constant, represent the needle wall, the surface of the needle, using Eq. (5), can be written as $R = \left(\frac{vax}{U}\right)^{1/2}$ which characterizes the shape and size of the needle.

Making use of similarity transformations given in (5) in equation (1) to (3), we get:

$$2\left(1 + \frac{1}{\beta}\right)(\eta f''' + f'') + f f'' = 0 \quad (6)$$

$$\eta\theta'' + \theta' + \frac{Pr}{2} f\theta' = 0 \quad (7)$$

The modified conditions on boundary are:

$$(a) = \frac{a\lambda}{2},\ f'(a) = \frac{\lambda}{2},\ \theta(a) = 1,$$

$$f'(\infty) = \frac{(1-\lambda)}{2},\ \theta(\infty) = 0 \quad (8)$$

where λ is the velocity ratio parameter, $Pr = \frac{\nu}{\alpha_0}$ denotes the Prandtl number.

The non-dimensional form of skin friction coefficient (C_f) and the heat transfer rate (Nusselt number (Nu)) are:

$$\sqrt{Re}\,C_f = 8\sqrt{a}\left(1 + \frac{1}{\beta}\right) f''(a) \text{ and}$$

$$\frac{Nu}{\sqrt{Re}} = -2\sqrt{a}\,\theta'(a) \quad (9)$$

3 Problem Solution

The set of differential Eqns. (6) and (7) are linearized by means of the successive linearization method (SLM), [17], [18]. The solution of these linearized equations is obtained by utilizing the Chebyshev collocation method. In SLM, it is supposed that the unidentified functions $F(\eta) = [f(\eta), \theta(\eta)]$ can be taken as:

$$F(\eta) = F_j(\eta) + \sum_{m=0}^{i-1} F_m(\eta), \quad (10)$$

where $F_j(\eta)$ $(j = 1,2, \ldots.)$ is undetermined function and $F_m(\eta)$ is an estimate. This estimate can be calculated by solving the linearized set of equations generated by applying equation (10) in the equations (6) and (7). The basic idea is that, even if j becomes large, F_j become very small and hence non-linear terms in F_j and their differential can be neglected.

Substituting (10) in the equations (6) to (7) and neglecting nonlinear terms containing, f_j, θ_j and ϕ_j, we get the following equations

$$a_1 f_j''' + a_2 f_j'' + a_3 f_j = r_1 \quad (11)$$

$$b_1 f_j + b_2 \theta_j'' + b_3 \theta_j' = r_2 \quad (12)$$

where

$a_1 = 2\eta[1 + \frac{1}{\beta}]$,

$a_2 = 2[1 + \frac{1}{\beta}] + \sum_{m=0}^{j-1} f_m$,

$a_3 = \sum_{m=0}^{j-1} f''$

$r_1 = -2\,\eta[1 + \frac{1}{\beta}]\sum_{m=0}^{j-1} f_m''' - 2[1 + \frac{1}{\beta}]\sum_{m=0}^{j-1} f_m'' - \sum_{m=0}^{i-1} f_m \sum_{m=0}^{j-1} f_m''$

$b_1 = \frac{Pr}{2}\sum_{m=0}^{j-1} \theta_m'$,

$b_2 = \eta$, $b_3 = 1 + \frac{Pr}{2}\sum_{m=0}^{j-1} f_m$,

$r_2 = -\frac{Pr}{2}\sum_{m=0}^{j-1} f_m \sum_{m=0}^{j-1} \theta_m' - \sum_{m=0}^{j-1} \theta_m' - \eta \sum_{m=0}^{j-1} \theta_m''$

The set of linearized equations (11) and (12) is solved by means of the Chebyshev collocation method, [19]. For this problem, the range of the solution$[0, \infty]$, is adjusted to [0, B], here B is a selected to obtain the conditions far away from the body. To implement this approach [0, B] is again changed to [-1, 1] by using the transformation:

$$\eta = \frac{(a+B)-(a-B)\xi}{2}, \quad -1 \le \xi \le 1 \quad (13)$$

The Gauss-Lobatto collocation points, [19], on [-1 1] are given by:

$$\xi_i = \cos\frac{\pi i}{N}, \quad i = 0,1,2,3 \ldots\ldots N \quad (14)$$

and f_j, θ_j and ϕ_j are estimated at the above points as:

$$f_j(\xi) = \sum_{k=0}^{N} f_j(\xi_k) T_k(\xi_i),$$
$$\theta_j(\xi) = \sum_{k=0}^{N} \theta_j(\xi_k) T_k(\xi_i), \quad (15)$$

where $T_k(\zeta)$ is the k^{th} order Chebyshev polynomial.

Similarly, the r^{th} differentials of f_j, and $\theta_j$are guesstimated as:

$$\frac{d^r f_j}{d\eta^r} = \sum_{k=0}^{N} D_{ki}^r f_j(\zeta_k),$$
$$\frac{d^r \theta_j}{d\eta^r} = \sum_{k=0}^{N} D_{ki}^r \theta_j(\zeta_k), \; i = 0,1,2 \ldots N \quad (16)$$

where $D = \frac{2}{L} D$ with D is the Chebyshev derivatives matrix.

Equations (15) - (16) are substituted into equations (11), and (12) to get the equation in matrix form as:

$$A_{j-1} X_j = R_{j-1} \quad (17)$$

where A_{j-1} represents order $2(N+1)$ square matrix and X_j and R_{j-1} represents order $2(N+1)$ column matrices given by:

$$A_{j-1} = \begin{bmatrix} A_{11} & A_{12} \\ A_{21} & A_{22} \end{bmatrix}, X_j = \begin{bmatrix} F_j \\ \Theta_j \end{bmatrix}, R_j = \begin{bmatrix} r_1 \\ r_2 \end{bmatrix} \quad (18)$$

Here

$F_j = \left[f_j(\xi_0), f_j(\xi_1), \ldots., f_j(\xi), f_j(\xi)\right]^T$,

$\Theta_j = \left[\theta_j(\xi_0), \theta_j(\xi_1), .., \theta_j(\xi_{N-1}), \theta_j(\xi)\right]^T$,

$A_{11} = a_1 D^3 + a_2 D^2 + a_3 I$, A12 = O,

$A_{21} = b_1 I$, $A_{22} = [b_2 D^2 + b_3 D]$

$r_1 = [r_1(\xi_1), r_1(\xi_2), r_1(\xi_3), \cdots, r_1(\xi_{N+1})]^T$,

$r_{2,} = [r_2(\xi_1), r_2(\xi_2), r_2(\xi_3), \cdots, r_2(\xi_{N+1})]^T$,

where the $[\ ]^T$ stands for transpose, O denotes the zero, I denotes the identity matrix.

Imposing the boundary conditions in terms of the collocation points, the solution is provided by:

$$X_j = A_{j-1}^{-1} R_{j-1} \quad (19)$$

4 Results and Discussion

The effects of three dimensionless parameters are primarily the focus of the current study. They are size of the needle (a), the Casson fluid parameter (β), and the velocity ratio parameter (λ). The effects of these parameters on the velocity and temperature together with a coefficient of skin friction and the heat transfer rate (Nusselt Number) are presented graphically (Figure 2, Figure 3, Figure 4, Figure 5 and Figure 6).

Figure 2 represents the impact of needle size on velocity and temperature profiles. The velocity increases as the size of the needle decreases, as depicted in Figure 2(a). Physically, as the thin

needle's size decreases, the surface area for the fluid particle decreases, lowering the force and thus increasing the velocity. Furthermore, as needle size is reduced, the boundary layer thickness for the velocity diminishes. The temperature and its boundary layer decrease with the thin needle size, as seen in Figure 2(b).

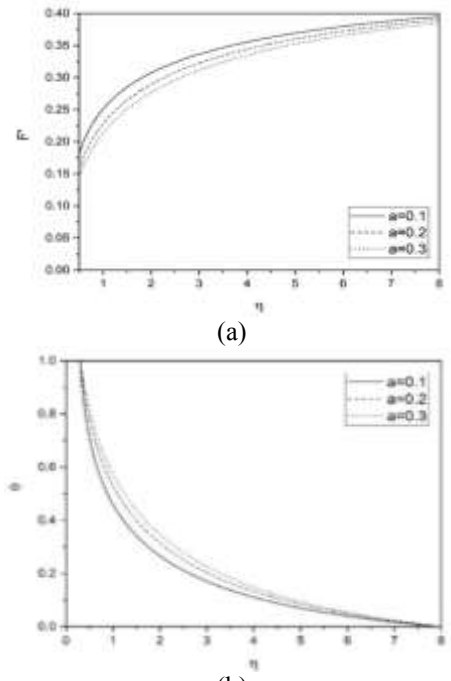

Fig. 2: "Effects of needle size on the (a) Velocity profile (b) Temperature Profile"

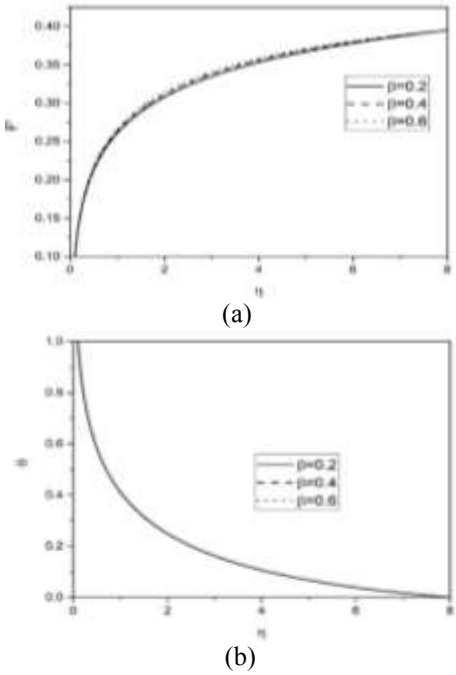

Fig. 3: "Effect of Casson fluid parameter on the (a) Velocity (b) Temperature"

The effect of the Casson fluid parameter (β**)** on the velocity and temperature is depicted in Figure 3. It is observed from Figure 3(a) that an increase in the value of β increases the velocity. Further, as η increases, the velocity also increases. The impact of β on the temperature is almost negligible as shown in Figure 3(b). It is clear that for increasing values of η, the temperature is decreasing.

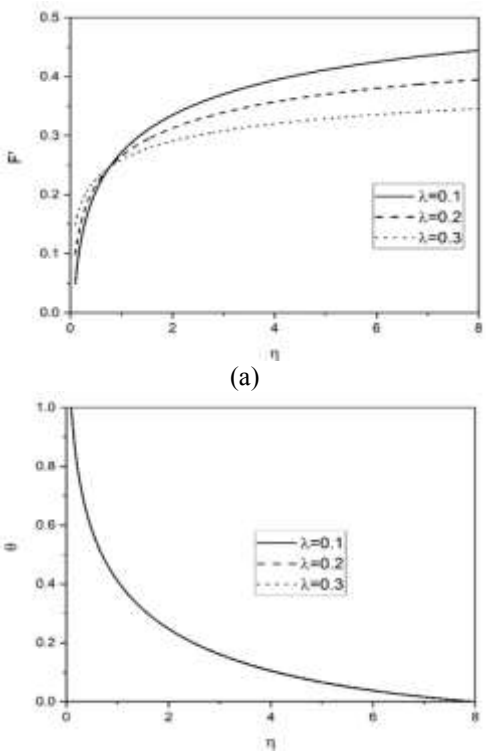

Fig. 4: Effect of velocity ratio parameter on the (a) Velocity (b) Temperature"

The variations in the velocity and temperature for different values of the velocity ratio parameter are presented in Figure 4. Figure 4(a) indicates that an increase in the value of λ enhances the velocity near the wall of the needle and subsequently decreases as it moves away from the needle's wall. As shown in Figure 4(b), the temperature is not affected by the velocity ratio parameter.

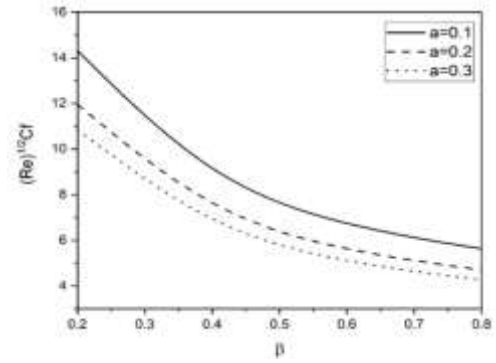

(a)

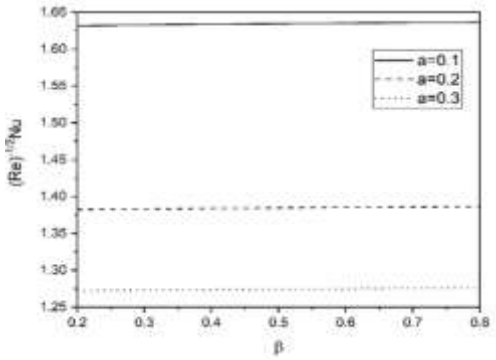

(b)

Fig. 5: "Effect of needle size on the (a) coefficient of skin friction (b) Heat transfer rate"

Figure 5 describes the influence of the size of the needle on the coefficient of skin friction and Nusselt number. According to Figure 5(a), for a constant value of needle size and an enhancing value of β, the skin friction decreases. In addition, as needle size increases, the skin friction coefficient decreases. The rate of heat transmission decreases as the needle size increases, as seen in Figure 5(b). The Casson fluid parameter has no substantial effect on the Nusselt number, as shown in Figure 5(b).

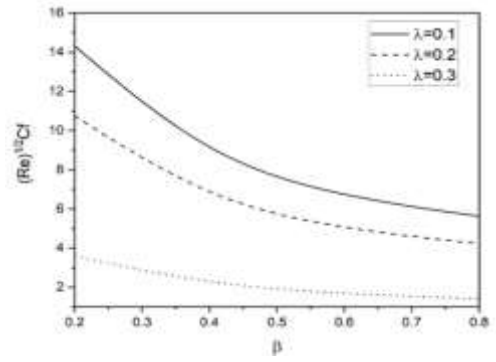

(a)

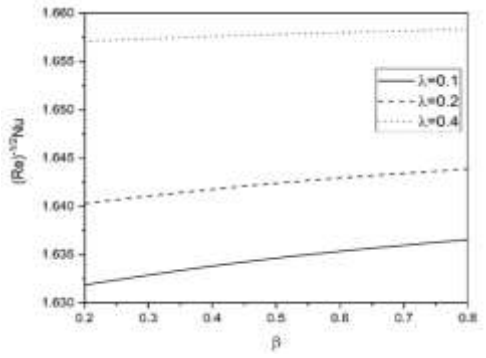

(b)

Fig. 6: "Effect of velocity ratio parameter on the (a) Skin friction coefficient (b) Heat transfer rate"

The consequence of the velocity ratio parameter on the coefficient of skin friction and Nusselt number is displayed in Figure 6. It is observed from Figure 6(a) that the skin friction coefficient is decreasing for enhancing values of the velocity ratio parameter. Figure 6(b) reveals that the rate of heat transfer is increasing with an increase in the velocity ration parameter.

5 Conclusion

The significance of flow parameters on the temperature, velocity, heat transfer rate, and the skin friction coefficient in the flow over a thin horizontal needle moving in a Casson fluid is examined. The main findings of the current examination are as follows

- The velocity rises with reducing needle size and drops with rising Casson fluid parameter.
- Temperature declines with the diminishing size of a thin needle. The effect of the Casson fluid and the velocity ratio parameters on the temperature are insignificant

The findings presented in this study open up intriguing possibilities for future research in the domain of fluid flow in porous media. This research explores a broader range of phenomena, including chemical reactions, Magnetic fields, heat source/sink, radiation, etc, which could provide a more comprehensive understanding of the complex systems.

References:

[1] Lee, L.L., *"Boundary layer over a thin needle"*, Phys. Fluids 10, 820–822, 1967.

[2] Narain, J.P. and Uberoi, M.S., *"Forced heat transfer over a thin needle"*, J. Heat Transf. Transactions of the ASME 94, 240-242, 1972.

[3] Narain, J.P. and Uberoi, M.S., *"Free-convection heat transfer from a thin vertical needle"*, Phys. Fluids 15,928–929, 1972.

[4] Narain, J.P. and Uberoi, M.S., *"Combined forced and free-convection over thin needles"*, International Journal of Heat and Mass Transfer 16.8 (1973): 1505-1512.

[5] Soid, S.K., Ishak, A., and Pop, I., Boundary layer flow past a continuously moving thin needle in a nanofluid, *Applied Thermal Engineering*, Vol 114, 2017, pp. 58-64.

[6] Qasim, M., Riaz, N., and Lu, D. Flow over a Needle Moving in a Stream of Dissipative Fluid Having Variable Viscosity and Thermal Conductivity. *Arab J Sci Eng.* 46, 7295–7302 (2021), https://doi.org/10.1007/s13369-021-05352-w.

[7] Prashar, P., Ojjela, O., and Kambhatla, P.K. Numerical investigation of boundary layer flow past a thin heated needle immersed in a hybrid nanofluid. *Indian J. Phys.*, 96, 137–150 (2022).

[8] Nazar, T., Bhatti, M.M. and Michaelides, E.E. Hybrid (Au-TiO2) nanofluid flow over a thin needle with magnetic field and thermal radiation: dual solutions and stability analysis, *Microfluid Nanofluid*, 26, 2 (2022).

[9] Casson, N. *"A flow equation for pigment-oil suspensions of the printing ink type."* In: Rheology of disperse systems, Mill CC (Ed.) Pergamon Press, Oxford, 22 (1959), 84–102.

[10] Souayeh, B., Reddy, M.G., Sreenivasulu, P., Poornima, T., Rahimi-Gorji, Md. e,f, Alarifi I.M., Comparative analysis on non-linear radiative heat transfer on MHD Casson nanofluid past a thin needle, *Journal of Molecular Liquids,* 284 (2019) 163–174.

[11] Bilal, M.; Urva, Y. Analysis of non-Newtonian fluid flow over a fine rotating thin needle for variable viscosity and activation energy. *SN Appl. Sci.* 2020, 2, 677.

[12] Ibrar, N., Reddy, M. G., Shahzad, S.A., Sreenivasulu, P. and Poornima, T., Interaction of single and multi-walls carbon nanotubes in magnetized-nano Casson fluid over the radiated horizontal needle. *SN Appl.* Sci. 2, 677 (2020).

[13] Akinshilo, A.T., Mabood, F., legbusi, A.O., Heat generation and nonlinear radiation effects on MHD Casson nanofluids over a thin needle embedded in a porous medium, *International Communications in Heat and Mass Transfer,* 127, (2021), 105547.

[14] Makanda, G. and Sibanda, P., Natural convection from a spinning cone in Casson fluid embedded in a porous medium with injection, temperature dependent viscosity and thermal conductivity, *WSEAS Transactions on Heat and Mass Transfer*, Vol. 12, pp. 11-20, 2017.

[15] Makanda, G. Shaw, S., Numerical analysis of the Bivariate Local Linearization Method (BLLM) for partial differential equations in Casson fluid flow, *WSEAS Transactions on Fluid Mechanics*, vol. 14, pp.132-141, 2019.

[16] Abayomi S. Oke, Belindar A. Juma, Anselm O. Oyem, Hydromagnetic Flow of Casson Fluid Carrying CNT and Graphene Nanoparticles in Armory Production, *WSEAS Transactions on Fluid Mechanics*, Vol. 18, 2023, pp.123-132, https://doi.org/10.37394/232013.2023.18.13.

[17] Makukula Z, Motsa SS, and Sibanda P (2010). On a new solution for the viscoelastic squeezing flow between two parallel plates. *Journal of Advanced Research in Applied Mathematics 2*(4), pp. 31-38.

[18] Makukula Z, Sibanda P, and Motsa SS (2010). A novel numerical technique for two-dimensional laminar flow between two moving porous walls. *Mathematical Problems in Engineering, Article ID 528956*, 15.

[19] C. Canuto, M. Y. Hussaini, A. Quarteroni, and T. A. Zang. *Spectral methods fundamentals in single domains*. Springer, Berlin, 2006

Contribution of Individual Authors to the Creation of a Scientific Article (Ghostwriting Policy)

The authors equally contributed to the present research, at all stages from the formulation of the problem to the final findings and solution.

Sources of Funding for Research Presented in a Scientific Article or Scientific Article Itself

No funding was received for conducting this study.

Conflicts of Interest

The authors declare no conflict of interest.

Creative Commons Attribution License 4.0 (Attribution 4.0 International, CC BY 4.0)

This article is published under the terms of the Creative Commons Attribution License 4.0
https://creativecommons.org/licenses/by/4.0/deed.en_US